HHS Public Access

Author manuscript

Mod Pathol. Author manuscript; available in PMC 2024 November 01.

Published in final edited form as:

Mod Pathol. 2023 November ; 36(11): 100305. doi:10.1016/j.modpat.2023.100305.

Comprehensive Molecular Characterization of Polymorphous Adenocarcinoma, Cribriform Subtype: Identifying Novel Fusions and Fusion Partners

Elan Hahn[1,2], **Bin Xu**[3], **Nora Katabi**[3], **Snjezana Dogan**[3], **Stephen M Smith**[2,4], **Bayardo Perez-Ordonez**[2,4], **Paras B Patel**[5], **Christina MacMillan**[1,2], **Daniel J Lubin**[6], **Jeffrey Gagan**[7], **Ilan Weinreb**[2,4], **Justin A Bishop**[7]

[1]Department of Pathology and Laboratory Medicine, Sinai Health System, Toronto, ON, Canada

[2]Department of Laboratory Medicine and Pathobiology, University of Toronto, ON, Canada

[3]Department of Pathology and Laboratory Medicine, Memorial Sloan Kettering Cancer Center, New York, NY, USA

[4]Laboratory Medicine Program, University Health Network, Toronto General Hospital, Toronto, ON, Canada

[5]ProPath, Dallas, TX, USA

[6]Department of Pathology and Laboratory Medicine, Emory University Hospital, Atlanta, GA, USA

[7]Department of Pathology, University of Texas Southwestern Medical Center, Dallas, TX, USA

Abstract

Polymorphous adenocarcinoma (PAC) is a common, usually low-grade salivary gland carcinoma. While conventional PACs are most associated with *PRKD1* p.E710D hotspot mutations, the cribriform subtype is often associated with gene fusions in *PRKD1*, *PRKD2*, or *PRKD3*. These fusions have been primarily identified by fluorescence in situ hybridization (FISH) analysis, with a minority evaluated by next generation sequencing (NGS). Many of the reported fusions were detected by break apart FISH probes and therefore have unknown partners, or were negative by FISH altogether. In this study, we aimed to further characterize the fusions associated with PAC with NGS. 54 PACs (exclusively cribriform and mixed/intermediate types to enrich for fusion-positive cases) were identified and subjected to NGS. 51 cases were successfully sequenced,

Corresponding author: Elan Hahn, Room 6A 120.03, 600 University Avenue, Toronto, Ontario, Canada, M5G 1X5, elan.hahn@sinaihealth.ca.

Author contributions:

E.H., I.W. and J.A.B. performed study concept and design; E.H., I.W., J.A.B., and J.G. performed development of methodology and writing, review and revision of the paper; B.X., N.K., S.D., S.M.S., B.P.O., P.B.P., C.M., and D.J.L. provided acquisition, analysis and interpretation of data. All authors read and approved the final paper.

Ethics Approval and Consent to Participate:

Institutional research ethics board approval was obtained from the represented institutions.

Conflict of Interest: None to declare.

28 of which demonstrated gene fusions involving *PRKD1*, *PRKD2*, or *PRKD3*. There were 10 cases with the *PRKD1* p.E710D mutation. We identified a diverse group of fusion partners, including 13 novel partners, 3 of which were recurrent. The most common partners for the *PRKD* genes were *ARID1A* and *ARID1B*. The wide variety of involved genes is unlike other salivary gland malignancies and warrants a broader strategy of sequencing for molecular confirmation for particularly challenging cases, as our NGS study shows.

Introduction

The field of head and neck pathology, specifically salivary gland pathology, has witnessed a brisk expansion of novel tumor entities as well as detailed molecular classification of known tumor entities. Examples of this expansion include the recently described microsecretory adenocarcinoma as well as the related microcribriform adenocarcinoma (1)(2). These tumors are not only tied together by regionally similar morphologies, but also by a shared molecular underpinning, namely *SS18* gene rearrangements. In a similar vein, polymorphous adenocarcinoma (PAC) is an entity with a unifying molecular pathogenesis. PAC predominantly affects the minor salivary glands, but has also been rarely identified in the parotid gland and other extraoral sites (3)(4)(5)(6)(7). PACs can demonstrate conventional fascicular or cribriform/glomerulopapillary patterns, or be mixed/indeterminate (3)(4)(5)(6)(7). Initially these tumors were described as low-grade adenocarcinomas with variable morphologies, which included papillary and cribriform patterns (3). Later, there was brief enthusiasm to separate tumors with prominent papillary and glomeruloid patterns into a separate tumor type known as cribriform adenocarcinoma (5)(6). Subsequent molecular analysis revealed that conventional PACs are most commonly associated with *PRKD1* p.E710D hotspot mutations, whereas the cribriform adenocarcinoma subtype is generally associated with fusions of *PRKD1*, *PRKD2*, or *PRKD3* (7)(8)(9). The segregation of molecular alteration category to histomorphologic subtype is modest, and interobserver reliability in characterizing histomorphologic subtypes is moderate, partly due to the high frequency of mixed/indeterminate tumors (9)(10). In the current WHO Classification of Head and Neck Tumors, classic/conventional and cribriform/papillary/glomeruloid tumors are regarded as subtypes of PAC. (11)

The PAC fusions have been primarily identified by fluorescence in situ hybridization (FISH) analysis, with only a small minority evaluated by next generation sequencing (NGS) (7). As a result, many of the reported fusions have unknown partners, or were negative by FISH altogether. In this study, we further characterize the genomic basis of the cribriform subtype of PAC, in addition to mixed/indeterminate tumors. If these specific molecular alterations ever contribute to prognosis and/or become targetable, it will become increasingly important for them to be sequenced and fully-characterized.

Materials/Subjects and Methods

Institutional research ethics board approval was obtained. Through a search of the laboratory information system (LIS), tumors diagnosed as PAC and classified as the cribriform subtype (n=35) or mixed/indeterminate (n=19) were reviewed for diagnosis confirmation by the

contributing author according to the paper by Xu *et al.* (10). Tumors were classified as cribriform subtype if they demonstrated predominantly cribriform architecture, or as mixed/indeterminate if they demonstrated non-focal (>5%) conventional growth. Pure conventional PACs were excluded to enrich the study for fusion-positive cases. Tumors were classified as high-grade if they demonstrated abundant mitotic activity and comedo-type necrosis.

RNA was isolated from formalin-fixed paraffin-embedded tissue, and complementary DNA (cDNA) synthesis was performed. In forty-seven cases, cDNA was captured from 1519 genes using IDT xGen hybrid capture probes and sequenced on a Nextseq 550 (Illumina) with at least 6 million reads per sample. Fusions were called by the StarFusion algorithm and manually confirmed in the Integrated Genomics Viewer (Broad Institute, Cambridge, USA) (12). The presence of *PRKD1* p.E710D hotspot mutations was also evaluated in the RNA sequencing data. In four cases, targeted RNA sequencing was performed using an anchored multiplex polymerase chain reaction (PCR)-based clinical molecular diagnostic assay (MSK-Archer FusionPlex) in a CLIA-accredited laboratory, to detect oncogenic fusion transcripts including a panel of 123 genes as previously described (13). In one case, the Trusight RNA Fusion Panel targeting 507 known fusion-related gene targets was used to prepare the library and sequenced using an Illumina MiSeq with approximately 3 million reads per sample. Fusion gene analysis was performed using the STAR and BOWTIE2 aligners and the Manta and JAFFA fusion callers (14)(15). Where FISH data were available through prior study, the fusions were confirmed retrospectively.

Results

A total of 54 cases were identified through LIS review. The patient ages ranged from 34 to 93 years, with an average of 60 years. There was a 3.5:1 female predominance (42 females and 12 males). The tumor sites included palate (n=18), pharynx (n=12), lip and oral cavity (n=11), parotid gland (n=7), and sinonasal and skull base (n=6) (Figure 1). The histologic spectrum of tumors includes cribriform subtype (n=35) and mixed/indeterminate tumors (n=19), ranging from unequivocal cribriform morphology to mixed conventional and cribriform morphologies, some with the cribriform component comprising only a minority of the tumor. (Figure 2)

NGS was successful in 51 cases. Thirteen cases were negative for both *PRKD1* p.E710D hotspot mutations and fusions involving *PRKD1*, *PRKD2*, or *PRKD3* (See supplementary data). The remaining 38 cases had positive molecular results. These include 28 cases with gene fusions, all of which involved *PRKD* genes (*PRKD1* n=23; *PRKD2* n=3; *PRKD3* n=2) (Table 1). There were 10 cases with the *PRKD1* p.E710D mutation.

A variety of novel fusion partners were identified (Table 1), with a recurrence of *ANXA7::PRKD1*, *GPHN::PRKD1,* and *ARID1B::PRKD1*. The latter of which, along with the previously recognized *ARID1A::PRKD1*, represented the most common fusion events in PAC (8 of 28 cases). Additionally, there was 1 high-grade cribriform variant that demonstrated 2 gene fusions, including *ARID1A::PRKD1* and a novel gene fusion (*ATP5F1A::SS18*). Overall, there were 17 fusion partners to *PRKD1*, *PRKD2*, and *PRKD3*,

including 13 novel partners. The fusions involved exons 11–13 of *PRKD1*, exons 10–11 of *PRKD2*, and exons 10–13 of *PRKD3* (Table 2).

Of the 35 tumors with cribriform patterns, 21 demonstrated gene fusions (60%), 6 were positive for the hotspot mutation (17%), and there were 8 negative cases (23%) (Figure 3). Of the 16 indeterminate cases that were successfully sequenced, 7 demonstrated gene fusions (44%), 4 demonstrated the *PRKD1* p.E710D hotspot mutation (25%), and 5 cases were negative (31%) (Figure 3).

Discussion

The discovery of the *PRKD1* p.E710D hotspot mutation in conventional PAC, followed by the discovery of fusions affecting *PRKD1*, *PRKD2*, and *PRKD3* in cribriform PAC, provided a molecular link between what was previously thought by some to represent two entities (8)(9). Indeed, both types are included under the umbrella diagnosis of PAC in the current WHO Classification of Head and Neck Tumors (11). Our results highlight the molecular diversity of PAC, comprising different molecular mechanisms of tumorigenesis (point mutations versus gene fusions) affecting a number of different genes, both within the PRKD family and their partners. Importantly, we describe multiple novel recurrent gene fusions in PACs. These include, *ANXA7::PRKD1*, *GPHN::PRKD1*, and *ARID1B::PRKD1* fusions, as detailed above.

Where available, the exonic breakpoints of each gene involved in the fusions were assessed (Table 2). The *PRKD* genes demonstrated consistent break points upstream of the protein kinase domain, the same domain affected by the activating E710D point mutation characteristic of conventional PAC. The *PRKD* genes share a common structure consisting of a 5’ regulatory cysteine-rich zinc-finger motif, an autoregulatory pleckstrin homology (PH) domain, and a protein kinase domain (Figure 4) (16)(17)(18)(19)(20)(21). The *PRKD* gene fusions recurrently occur in regions that preserve the protein kinase domain while removing the cysteine rich regulatory domain and either disrupting or removing the PH domain (exons 11–13 of *PRKD1*, exons 10–11 of *PRKD2*, exons 10–13 of *PRKD3*) (Figure 4). Further, deletion of all or part of the PH domain has been shown to increase basal kinase activity in *PRKD1*, and likely acts similarly in *PRKD2* and *PRKD3* (16). Additionally, a specific amino acid residue (T513) in PKD1, that when mutated loses its autoregulatory function, is lost in all of our *PRKD1* fusion-positive cases where exon-level data was available (22).

The diverse gene partners included genes that have a wide variety of cellular functions. *ARID1A*, the most common recurrent fusion identified, only had fusion breakpoints observed in the first intron. This region is far upstream of any functional domains and commonly occurring deactivating mutations in cancers (23)(24)(25). The breakpoints described on *ARID1B* are also upstream of the ARID domain (26). A number of other gene partners in our cohort featured intron 1 fusion breakpoints (*ACTN1*, *CTNNB1*, and *RBPMS*). It is unlikely that any biochemical activity is gained from these 5’ fusion partners. In other instances, however, more of the functional domains are included in the fusions (*ATL2*, *ERC1*, *NFIA*, *SS18*, *TAX1BP1*, and *KTN1*). Considering the diversity of gene

partners and the most commonly recurrent fusion contributing only one exon, the fusions likely function by the contribution of a promoter or enhancer from the first gene partner to the protein kinase domain of the *PRKD* gene, in addition to removing the cysteine-rich zinc-finger regulatory domain and inactivating the auto regulatory PH domain of the *PKRD* gene, through complete removal or disruption of its function. Beyond this, the contribution of the 5' partner, if any, is unknown.

We identified 2 cases with a novel *ARID1B::PRKD1* gene fusion. When taken in the context of the well described *ARID1A::PRKD1* fusions in these tumors, fusion events involving this family of genes appear to characterize the most common rearrangements in PAC. We also describe the first fusions partners for *PRKD2* (*CTNNB1*, *RBPMS*, and *SS18*). Additionally, in our study, we identified 2 cases with fusions involving the *PRKD3* gene, both of which have *ATL2* as the fusion partner. This finding has been described before, and perhaps characterizes the extent of *PRKD3* fusions seen in PAC (27).

Interestingly, we identified 2 tumors with fusions involving the *SS18* gene. One of these tumors was high-grade, and demonstrated 2 fusions: the canonical *ARID1A::PRKD1* fusion, as well as an *ATP5F1A::SS18* fusion. Morphologically, the tumor had high-grade areas in addition to areas that were similar to microsecretory adenocarcinoma (Figure 5A). The possible explanations for this case include a single tumor with 2 gene fusions and high-grade transformation, or alternatively, a collision tumor between a high-grade polymorphous adenocarcinoma and a microsecretory adenocarcinoma. The other tumor demonstrated a single fusion between *SS18* and *PRKD2*, a novel finding in our study. Within this tumor there were foci that demonstrated luminal secretions reminiscent of microsecretory adenocarcinoma (Figure 5B). This case raises the possibility that the distinction between these two tumors may not be as clear as initially described. Both entities are frequently located in the oral cavity, and demonstrate bland cytology and infiltrative, occasionally single-filed, growth, with a shared immunophenotype (1). This case also highlights a potential pitfall of relying solely on FISH analysis for molecular diagnosis.

Histomorphologic characterization segregates tumors by molecular alteration with modest reliability, with conventional/fascicular tumors typically harboring *PRKD1* hotspot mutations, and those with cribriform morphologies harboring fusions involving *PRKD1*, *PRKD2*, and *PRKD3* (7). There are frequent exceptions to this rule, however, as is demonstrated by our data, which further brings into question the value of routine histologic subtyping. Interobserver reliability has been demonstrated to be moderate in histomorphologically characterizing these tumors (10). In the current clinical workflow, the use of histomorphology alone is generally sufficient for diagnostic accuracy as it pertains to clinical management. Laboratories with NGS panels that do not include *PRKD1*, *PRKD2*, or *PRKD3*, may be able to target one of the above described fusion partners to confirm a diagnosis of PAC in difficult cases. Should one of the molecular alterations be proven targetable, histomorphology alone will be insufficient, and molecular testing of all PAC cases will be necessary in the identification of these alterations.

Conclusion

NGS of cribriform and mixed/indeterminate PAC has elucidated a wide variety of gene fusions, including entirely novel fusions, and multiple PRKD gene partners, in addition to a non-negligible number of *PRKD1* p.E710D hotspot-mutated tumors. The most common partners for *PRKD1* are *ARID1A* and *ARID1B*, while *PRKD3* seems to preferentially associate with *ATL2*. Two PAC cases showed *SS18* fusions highlighting that this gene is not specific for microsecretory or microcribriform adenocarcinomas. The wide variety of involved genes is unlike other salivary gland malignancies that are typically characterized by one or two canonical fusions, and warrants a broader strategy of sequencing for diagnostic fusion confirmation. As we trudge further into the era of personalized medicine and targeted therapies, our results highlight the need for more comprehensive molecular analysis to fully elucidate pathogenic fusions in these tumors.

Supplementary Material

Refer to Web version on PubMed Central for supplementary material.

Funding:

Research reported in this publication was supported in part by the Cancer Center Support Grant of the National Institutes of Health/National Cancer Institute under award number P30 CA008748 (BX, NK, SD).

Data availability statement:

The datasets used and/or analyzed during the current study are available from the corresponding author on reasonable request. The majority of the data generated or analyzed during this study are included in this published article and its supplementary information files.

References

1. Bishop JA, Weinreb I, Swanson D, Westra WH, Qureshi HS, Sciubba J, et al. Microsecretory Adenocarcinoma: A Novel Salivary Gland Tumor Characterized by a Recurrent MEF2C-SS18 Fusion. Am J Surg Pathol. 2019 Aug;43(8):1023–32. [PubMed: 31094920]
2. Weinreb I, Hahn E, Dickson BC, Rooper LM, Rupp NJ, Freiberger SN, et al. Microcribriform Adenocarcinoma of Salivary Glands: A Unique Tumor Entity Characterized by an SS18::ZBTB7A Fusion. Am J Surg Pathol. 2023 Feb 1;47(2):194–201. [PubMed: 36221318]
3. Evans HL, Batsakis JG. Polymorphous low-grade adenocarcinoma of minor salivary glands. A study of 14 cases of a distinctive neoplasm. Cancer. 1984 Feb 15;53(4):935–42. [PubMed: 6692293]
4. Evans HL, Luna MA. Polymorphous low-grade adenocarcinoma: a study of 40 cases with long-term follow up and an evaluation of the importance of papillary areas. Am J Surg Pathol. 2000 Oct;24(10):1319–28. [PubMed: 11023093]
5. Michal M, Skálová A, Simpson RH, Raslan WF, Curík R, Leivo I, et al. Cribriform adenocarcinoma of the tongue: a hitherto unrecognized type of adenocarcinoma characteristically occurring in the tongue. Histopathology. 1999 Dec;35(6):495–501. [PubMed: 10583573]
6. Skalova A, Sima R, Kaspirkova-Nemcova J, Simpson RHW, Elmberger G, Leivo I, et al. Cribriform adenocarcinoma of minor salivary gland origin principally affecting the tongue: characterization of new entity. Am J Surg Pathol. 2011 Aug;35(8):1168–76. [PubMed: 21716087]

7. Sebastiao APM, Xu B, Lozada JR, Pareja F, Geyer FC, Da Cruz Paula A, et al. Histologic spectrum of polymorphous adenocarcinoma of the salivary gland harbor genetic alterations affecting PRKD genes. Mod Pathol Off J U S Can Acad Pathol Inc. 2020 Jan;33(1):65–73.
8. Weinreb I, Zhang L, Tirunagari LMS, Sung YS, Chen CL, Perez-Ordonez B, et al. Novel PRKD gene rearrangements and variant fusions in cribriform adenocarcinoma of salivary gland origin. Genes Chromosomes Cancer. 2014 Oct;53(10):845–56. [PubMed: 24942367]
9. Weinreb I, Piscuoglio S, Martelotto LG, Waggott D, Ng CKY, Perez-Ordonez B, et al. Hotspot activating PRKD1 somatic mutations in polymorphous low-grade adenocarcinomas of the salivary glands. Nat Genet. 2014 Nov;46(11):1166–9. [PubMed: 25240283]
10. Xu B, Barbieri AL, Bishop JA, Chiosea SI, Dogan S, Di Palma S, et al. Histologic Classification and Molecular Signature of Polymorphous Adenocarcinoma (PAC) and Cribriform Adenocarcinoma of Salivary Gland (CASG): An International Interobserver Study. Am J Surg Pathol. 2020 Apr;44(4):545–52. [PubMed: 31917707]
11. Skalova A, Thompson LDR, Bishop JA, Mehrotra R, Hyrcza MD. Salivary gland tumours. In: Board WCTE, editor. Head and neck tumours. 5th ed. Lyon: International Agency for Research on Cancer; 2022.
12. Haas BJ, Dobin A, Li B, Stransky N, Pochet N, Regev A. Accuracy assessment of fusion transcript detection via read-mapping and de novo fusion transcript assembly-based methods. Genome Biol. 2019 Oct 21;20(1):213. [PubMed: 31639029]
13. Zhu G, Benayed R, Ho C, Mullaney K, Sukhadia P, Rios K, et al. . Diagnosis of known sarcoma fusions and novel fusion partners by targeted RNA sequencing with identification of a recurrent ACTB-FOSB fusion in pseudomyogenic hemangioendothelioma. Mod Pathol Off J U S Can Acad Pathol Inc. 2019 May;32(5):609–20.
14. Liu S, Tsai WH, Ding Y, Chen R, Fang Z, Huo Z, et al. Comprehensive evaluation of fusion transcript detection algorithms and a meta-caller to combine top performing methods in paired-end RNA-seq data. Nucleic Acids Res. 2016 Mar 18;44(5):e47. [PubMed: 26582927]
15. Chen X, Schulz-Trieglaff O, Shaw R, Barnes B, Schlesinger F, Källberg M, et al. Manta: rapid detection of structural variants and indels for germline and cancer sequencing applications. Bioinforma Oxf Engl. 2016 Apr 15;32(8):1220–2.
16. Iglesias T, Rozengurt E. Protein kinase D activation by mutations within its pleckstrin homology domain. J Biol Chem. 1998 Jan 2;273(1):410–6. [PubMed: 9417097]
17. Sturany S, Van Lint J, Muller F, Wilda M, Hameister H, Hocker M, et al. Molecular cloning and characterization of the human protein kinase D2. A novel member of the protein kinase D family of serine threonine kinases. J Biol Chem. 2001 Feb 2;276(5):3310–8. [PubMed: 11062248]
18. Hayashi A, Seki N, Hattori A, Kozuma S, Saito T. PKCnu, a new member of the protein kinase C family, composes a fourth subfamily with PKCmu. Biochim Biophys Acta. 1999 May 6;1450(1):99–106. [PubMed: 10231560]
19. Steinberg SF. Regulation of protein kinase D1 activity. Mol Pharmacol. 2012 Mar;81(3):284–91. [PubMed: 22188925]
20. Zhou X, Edmonson MN, Wilkinson MR, Patel A, Wu G, Liu Y, et al. Exploring genomic alteration in pediatric cancer using ProteinPaint. Nat Genet. 2016 Jan;48(1):4–6. [PubMed: 26711108]
21. UniProt Consortium. UniProt: the Universal Protein Knowledgebase in 2023. Nucleic Acids Res. 2023 Jan 6;51(D1):D523–31. [PubMed: 36408920]
22. Ziemba BP, Pilling C, Calleja V, Larijani B, Falke JJ. The PH domain of phosphoinositide-dependent kinase-1 exhibits a novel, phospho-regulated monomer-dimer equilibrium with important implications for kinase domain activation: single-molecule and ensemble studies. Biochemistry. 2013 Jul 16;52(28):4820–9. [PubMed: 23745598]
23. Wu JN, Roberts CWM. ARID1A mutations in cancer: another epigenetic tumor suppressor? Cancer Discov. 2013 Jan;3(1):35–43. [PubMed: 23208470]
24. Guan B, Mao TL, Panuganti PK, Kuhn E, Kurman RJ, Maeda D, et al. Mutation and loss of expression of ARID1A in uterine low-grade endometrioid carcinoma. Am J Surg Pathol. 2011 May;35(5):625–32. [PubMed: 21412130]
25. Cornen S, Adelaide J, Bertucci F, Finetti P, Guille A, Birnbaum DJ, et al. Mutations and deletions of ARID1A in breast tumors. Oncogene. 2012 Sep 20;31(38):4255–6. [PubMed: 22249247]

26. Hurlstone AFL, Olave IA, Barker N, van Noort M, Clevers H. Cloning and characterization of hELD/OSA1, a novel BRG1 interacting protein. Biochem J. 2002 May 15;364(Pt 1):255–64. [PubMed: 11988099]

27. Freiberger SN, Brada M, Fritz C, Höller S, Vogetseder A, Horcic M, et al. . SalvGlandDx - a comprehensive salivary gland neoplasm specific next generation sequencing panel to facilitate diagnosis and identify therapeutic targets. Neoplasia N Y N. 2021 May;23(5):473–87.

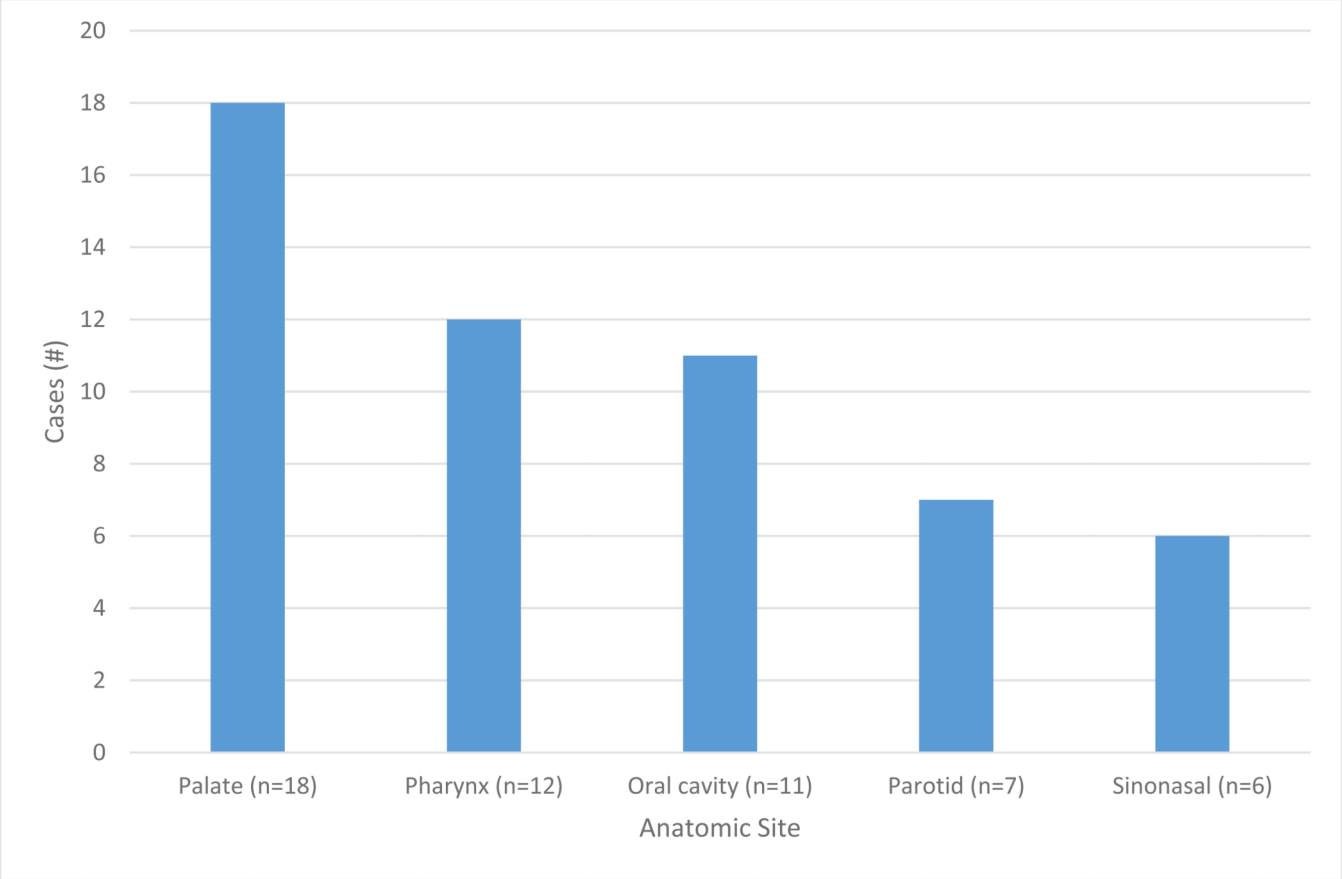

Figure 1:
Number of cases by anatomic site.

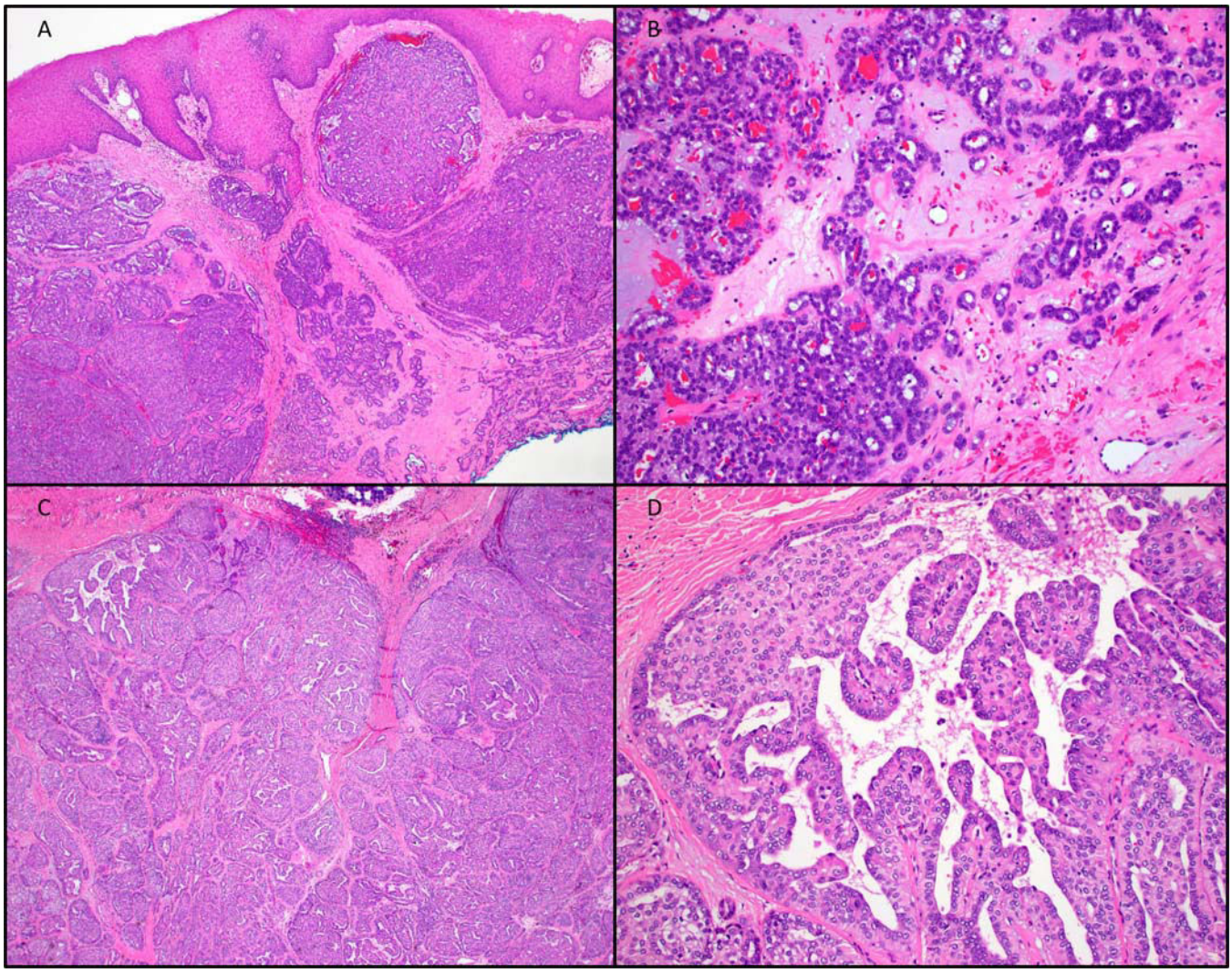

Figure 2:

A. Low-power view of a mixed/indeterminate subtype tumour of the minor salivary glands with a *PRKD1* E710D hotspot mutation. B. High-power view of a conventional focus. C. Low-power and D. high-power views of a cribriform subtype tumor of the parotid gland with a *KTN1::PRKD1* fusion.

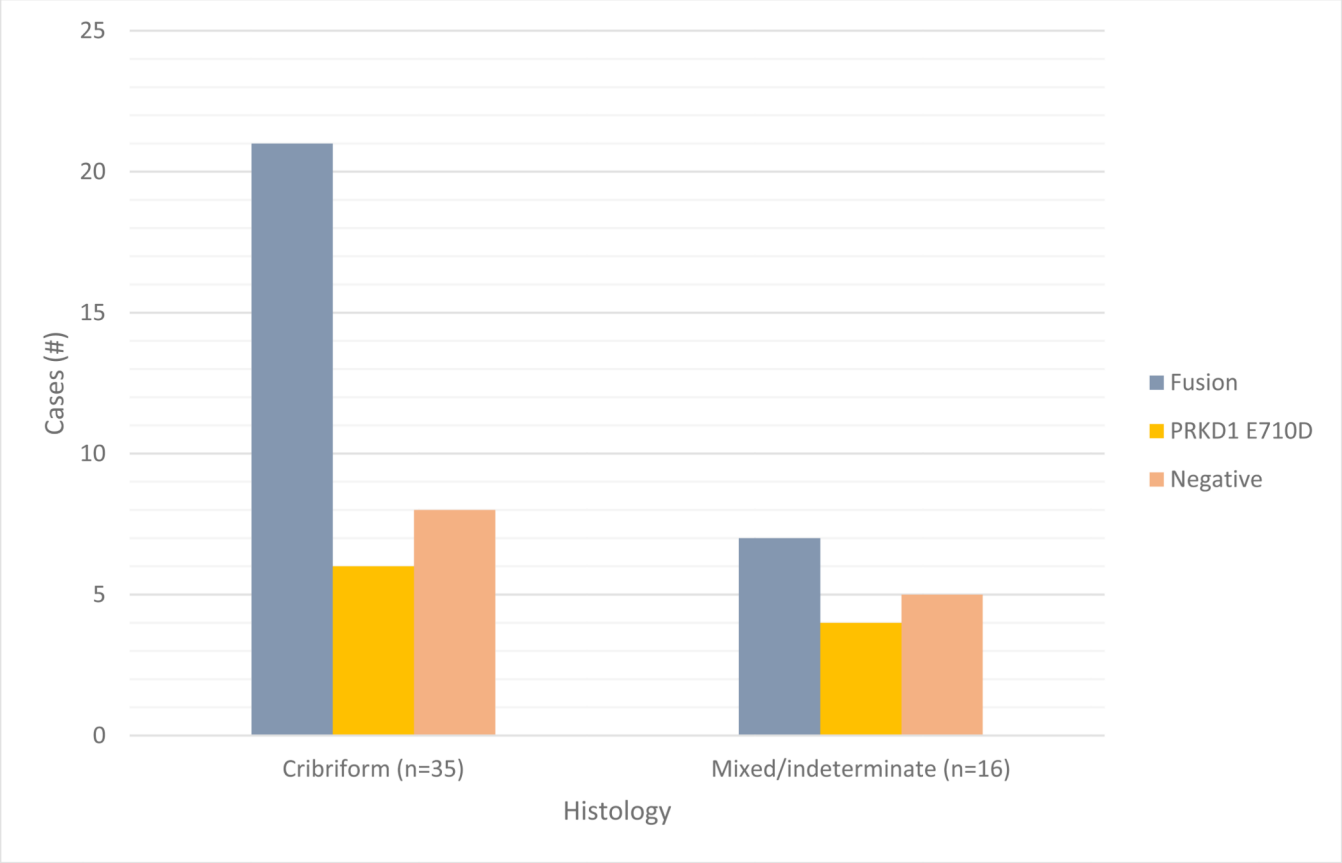

Figure 3:
Molecular alterations arranged by histomorphologic subtype.

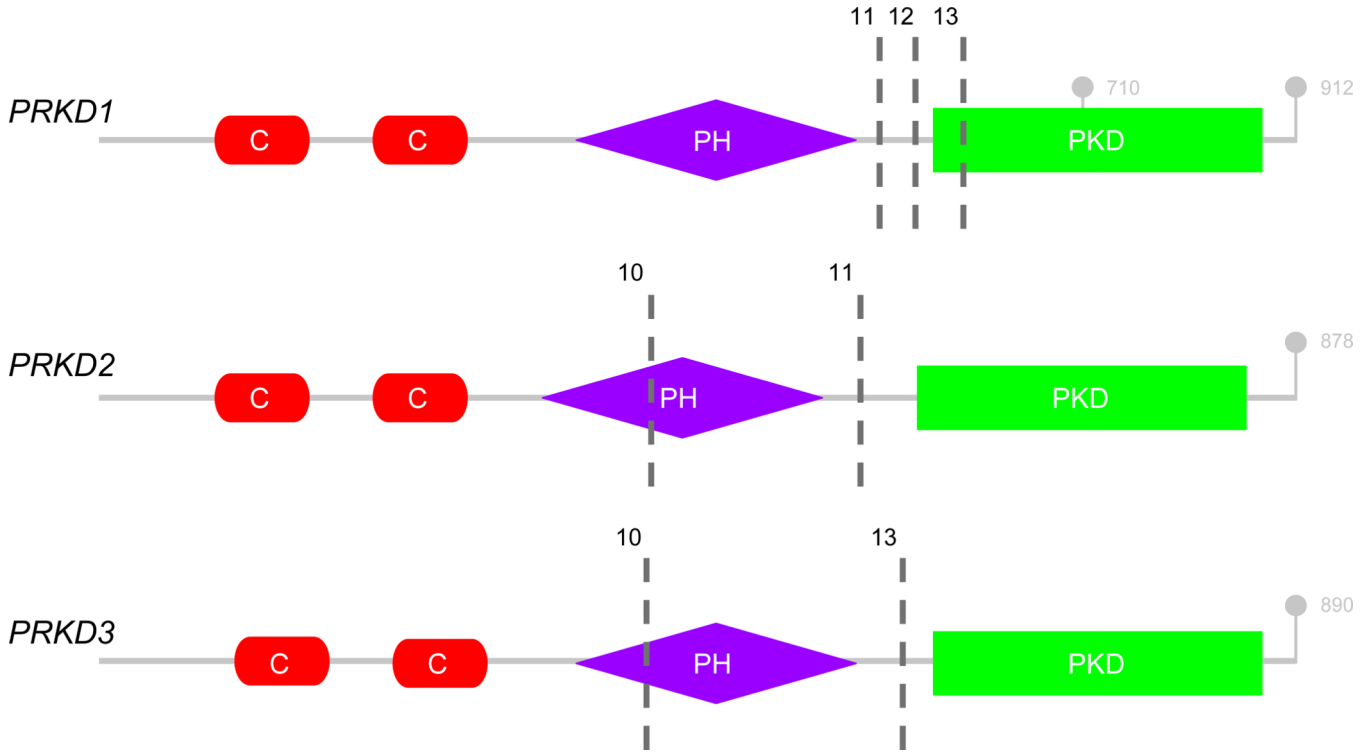

Figure 4:

Structure of the *PRKD* genes. Cysteine-rich regulatory domains (red; C); pleckstrinhomology domain (purple; PH); protein kinase domain (green; PKD). Exonic breakpoints found in our cohort denoted by hashed black bars (exons 11, 12 and 13 in *PRKD1*; exons 10 and 11 in *PRKD2*; exons 10 and 13 in *PRKD3*). Terminal codons and E710 hot-spot indicated in gray (21)(22).

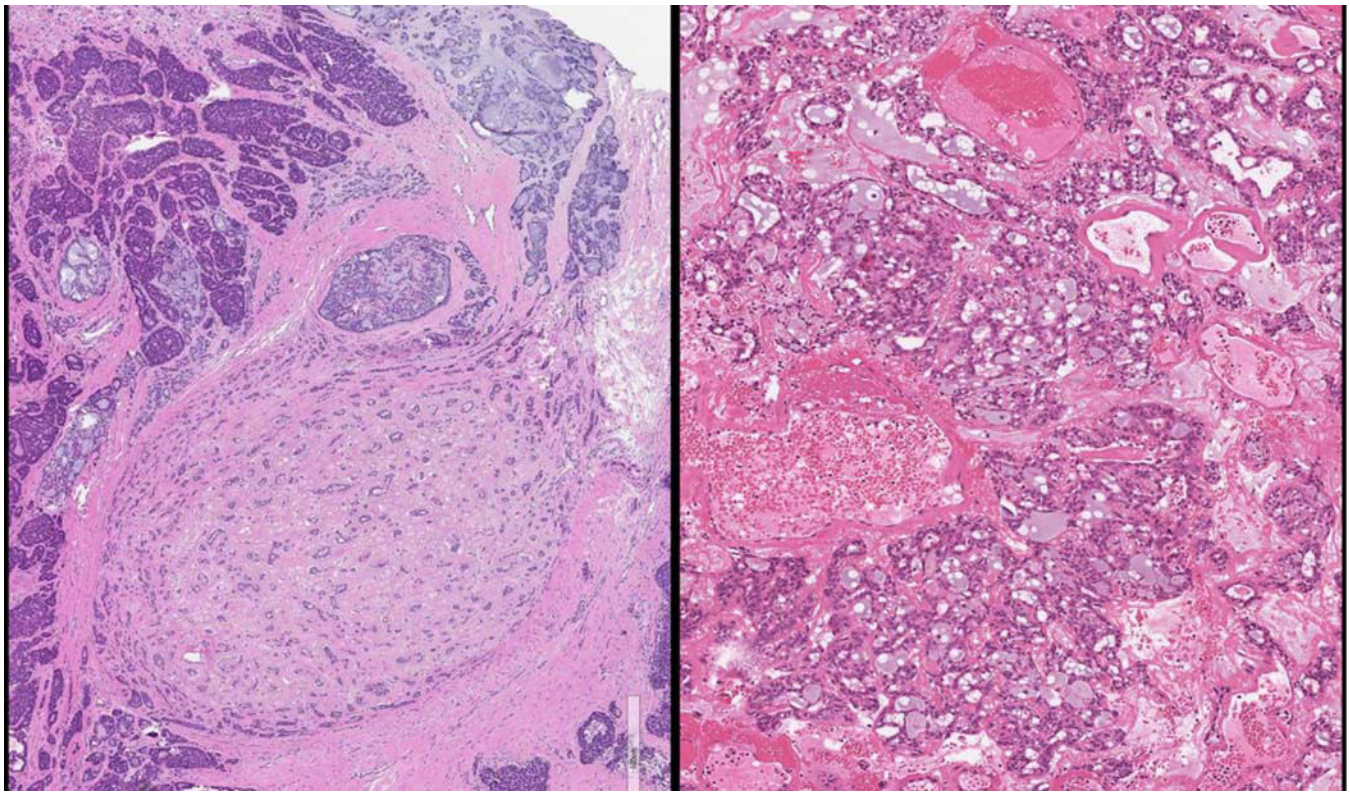

Figure 5:

A. Tumor with *ARID1A::PRKD1* and *ATP5F1A::SS18* fusions, demonstrating both high-grade areas and areas morphologically reminiscent of microsecretory adenocarcinoma.

B. *SS18::PRKD2* fusion-positive tumor, also with foci reminiscent of microsecretory adenocarcinoma.

Table 1:

Demographic, histomorphologic, and molecular findings of the fusion-positive cases. Novel fusions are bolded. Not available listed as "-".

Age	Sex	Location	Histology	Grade	Mutation	Fusion
53	F	Parotid	Cribriform	High	–	***ACTN1::PRKD1***
48	F	Palate	Mixed/indeterminate	Low	–	***ANXA7::PRKD1***
91	F	Oral cavity	Mixed/indeterminate	Low	–	***ANXA7::PRKD1***
49	M	Pharynx	Cribriform	Low	Negative	*ARID1A::PRKD1*
66	F	Pharynx	Cribriform	Low	Negative	*ARID1A::PRKD1*
63	F	Pharynx	Cribriform	Low	–	*ARID1A::PRKD1*
38	F	Oral cavity	Cribriform	Low	–	*ARID1A::PRKD1*
37	F	Pharynx	Cribriform	Low	–	*ARID1A::PRKD1*
57	F	Sinonasal	Cribriform	High	Negative	*ARID1A::PRKD1 and* ***ATP5F1A::SS18***
45	F	Sinonasal	Cribriform	–	–	***ARID1B::PRKD1***
46	F	Parotid	Cribriform	Low	–	***ARID1B::PRKD1***
46	F	Parotid	Cribriform	Low	Negative	*DDX3X::PRKD1*
34	F	Pharynx	Cribriform	Low	–	***ERC1::PRKD1***
38	F	Sinonasal	Mixed/indeterminate	–	–	***GPHN::PRKD1***
47	F	Palate	Cribriform	–	–	***GPHN::PRKD1***
46	M	Sinonasal	Mixed/indeterminate	Low	–	*KTN1::PRKD1*
63	F	Pharynx	Cribriform	Low	–	*KTN1::PRKD1*
78	M	Parotid	Cribriform	–	–	*KTN1::PRKD1*
68	F	Palate	Mixed/indeterminate	Low	–	***NFIA::PRKD1***
66	F	Oral cavity	Cribriform	High	–	***NOL4L::PRKD1***
48	F	Oral cavity	Mixed/indeterminate	–	–	***RBM25::PRKD1***
47	F	Palate	Cribriform	–	–	***TAX1BP1::PRKD1***
43	M	Palate	Cribriform	High	–	***UBE2D3::PRKD1***
65	F	Pharynx	Cribriform	Low	–	***CTNNB1::PRKD2***
75	M	Palate	Cribriform	Low	–	***RBPMS::PRKD2***
84	F	Pharynx	Cribriform	Low	–	***SS18::PRKD2***
39	F	Pharynx	Cribriform	Low	–	*ATL2::PRKD3*

Age	Sex	Location	Histology	Grade	Mutation	Fusion
59	F	Palate	Mixed/indeterminate	Low	–	*ATL2::PRKD3*

Table 2:

Exonic breakpoints of a subset of fusion-positive cases.

Fusion	Gene A	Gene A exon	Gene B	Gene B exon
ARID1B::PRKD1	*ARID1B*	4	*PRKD1*	11
KTN1::PRKD1	*KTN1*	41	*PRKD1*	11
NOL4L::PRKD1	*NOL4L*	2	*PRKD1*	11
RBM25::PRKD1	*RBM25*	2	*PRKD1*	11
ACTN1::PRKD1	*ACTN1*	1	*PRKD1*	12
ANXA7::PRKD1	*ANXA7*	5	*PRKD1*	12
ARID1A::PRKD1	*ARID1A*	1	*PRKD1*	12
UBE2D3::PRKD1	*UBE2D3*	4	*PRKD1*	12
ANXA7::PRKD1	*ANXA7*	5	*PRKD1*	13
ARID1A::PRKD1	*ARD1A*	1	*PRKD1*	13
ARID1A::PRKD1	*ARID1A*	1	*PRKD1*	13
ARID1B::PRKD1	*ARID1B*	4	*PRKD1*	13
ERC1::PRKD1	*ERC1*	13	*PRKD1*	13
GPHN::PRKD1	*GPHN*	8	*PRKD1*	13
GPHN::PRKD1	*GPHN*	8	*PRKD1*	13
KTN1::PRKD1	*KTN1*	33	*PRKD1*	13
KTN1::PRKD1	*KTN1*	33	*PRKD1*	13
NFIA::PRKD1	*NFIA*	11	*PRKD1*	13
TAX1BP1::PRKD1	*TAX1BP1*	8	*PRKD1*	13
CTNNB1::PRKD2	*CTNNB1*	1	*PRKD2*	10
RBPMS::PRKD2	*RBPMS*	1	*PRKD2*	11
SS18::PRKD2	*SS18*	10	*PRKD2*	11
ATL2::PRKD3	*ATL2*	12	*PRKD3*	10
ATL2::PRKD3	*ATL2*	11	*PRKD3*	13